LA-UR-19-20354
Approved for public release; distribution is unlimited.

Title: Explosion Source Models and the Scattering Origin of Regional Phases from SPE Phase 1 Coda Spectral Ratios

Author(s): Phillips, William Scott
Patton, Howard John
Cleveland, Kenneth Michael
Larmat, Carene

Intended for: Report

Issued: 2019-01-17

Explosion Source Models and the Scattering Origin of Regional Phases from SPE Phase 1 Coda Spectral Ratios

Monitoring Implications –Discrimination and Yield Estimation

Trimmed version of LA-UR-18-31678

W.S. Phillips, H.J. Patton, K.M. Cleveland, C. Larmat
Los Alamos National Laboratory
January 8, 2019

Abstract

The Source Physics Experiment (SPE) explosions provide comprehensive ground truth information, and near-source recordings that are rarely available in typical monitoring scenarios. Here, we analyze these data together with local and regional distance recordings to isolate source and propagation effects, and to potentially improve monitoring at distance. We examine source spectral ratios, which can be measured to high precision by taking advantage of many SPE and independently operated stations, as well as the redundancy available from coda waves. Classical source models (Mueller and Murphy, 1971, MM71; Denny and Johnson, 1991, DJ91) predict the source ratios poorly; however, a hybrid model (MM71 with DJ91 cavity radii) performs better. We observe a distinct spectral modulation at 6-9 Hz that is not predicted by classical models, most likely caused by short period surface waves (Rg) interfering with those produced by spallation of near surface layers. The same modulation is observed for compressional (P) and shear (S) waves at distance, indicating that local and regional phases originate as near-source Rg that is scattered into body waves. The scattering process must be accounted for quantitatively to best use remotely recorded signals to monitor treaty compliance, discriminate event types, and estimate explosion yields over broad regions.

Introduction

An important goal of explosion monitoring research is to enable broad area discrimination, yield estimation, and further characterization of foreign nuclear tests. The term "broad area" implies that source, and propagation effects are accurately known and can be accounted for beyond the well-studied, historical test sites. As models are improved using new data, simulations, and physical understanding, we test transportability using ground truth information, leading to next level understanding, whereupon the process can be repeated. The SPE experiments are important to this process, as they allow us to examine source region data along with data from more typical monitoring offsets, and include ground truth, to test current models and physical understanding of source and propagation effects.

In the following we will examine source spectral ratios of SPE experiments, which can be measured to high precision, to test classical source models, develop new models, and to understand the generation of local and regional phases.

Research Accomplished

Data

We examined SPE seismic data visually to identify phases in traditional ways, and observations are summarized by Phillips and Stead, this volume. Observations relevant to source and path waveform studies include: 1) far-field (near-source surface) records are dominated by Rg and Rg coda below 10 Hz, and by P and P coda above, 2) near-local distance high frequency waveforms are fairly featureless after the direct P, very different from what would be expected from earthquake sources, likely due to strong Rg and Rg-to-Rg scattering, and 3) distinct shear phases begin to emerge at roughly 100 km.

In addition, we discovered amplitude inconsistencies between events for individual stations and channels that could result from gain recording mistakes or temporal site effect issues. To mitigate, we simply discarded stations that did not fit the main trend. This could lead to slight errors in the overall level of the spectral ratios we present, but should not affect frequency dependence.

Method

Taking coda spectral ratios is a fairly simple procedure. Envelopes are created according to the "GNEM CodaMag" standard adopted by the national laboratories and AFTAC. The only issue to watch out for is filtering when sample rate is high and the filter band is low. In such cases we apply decimation with FIR anti-alias filters, such as those found in SAC. Decimation also stabilizes the enveloping procedure. The normal method is to correct for instrument response, and we use the entire response that includes anti-aliasing filters that are applied during initial down sampling in order to take advantage of the highest frequency ranges. Because the SPE instrument responses could not be trusted, we did the problem with and without applying responses and made sure results matched. Note that instrument responses are important only if instrument calibrations change with time for a given station and channel. Sample rates for the geophone array topped out at 500 Hz, so we ran narrow, sub-octave bands up to 200 Hz. Array envelopes are stacked, as are horizontal components. We also compute R and T envelopes, rotating when needed.

Once envelopes are in place, we simply take point by point differences between pairs of events for the same station, channel and band, requiring SNR greater than 2 for both (Figure 1). For

near-source envelopes, measurements are dominated by Rg plus Rg coda, or by P plus P coda, depending on band as discussed above. For regional distance stations, we measured P and S windows separately. Note that regional S dies out faster than P at high frequencies, and the S measurement becomes a late P coda spectral ratio. This is easy to diagnose, and we have not made any effort to exclude these measurements from display. Spectral ratios have eliminated common path and site effects, and we stack differencing results for many stations and channels for each event pair.

Results

Spectral ratios are shown for all SPE event pairs in matrix format in Figure 2. Error bars are also shown, these represent twice the standard deviation of the results as measured by the MADn of the stacked stations and channels.

Ratios are formed with the higher yield event in the numerator, lower yield in the denominator. This results in sigmoid shapes, with the low bands representing the moment ratio, and the downward and recovering bends are the corner frequencies of the larger and smaller events, respectively. The SPE spectral ratios are complicated by a distinctive modulation between 6 and 9 Hz, especially apparent for event pairs that differ greatly in yield.

We plot results for Z, R, and T channels, all of which overlay each other. This is not surprising as all channels contain homogenizing, out of plane scattering of all wave types. In particular, we cannot associate Z and T channels with P and S, respectively. We will discuss this further in the "Fisk Conjecture" section.

Results for SPE-2 / SPE-1 match the spectral ratios presented by Ford and Walter (2013), as determined using illustration software to overlay and distort graphics to match axes.

Comparing SPE-2 and SPE-3 gives an extremely flat ratio. These events were placed at the same depth, and were designed to have similar yields. The motivation was to test the effect that SPE-2 damage would have on SPE-3 records. We see a tiny lowering of the ratio at and above 100 Hz, which is the right direction to be associated with damping due to the damage, but it is difficult to argue that this is significant.

Once SPE-5 was successfully performed, we had the opportunity to compare two events of different yields at regional distances. These spectral ratios were separated into P and S portions of the envelope, as shown in Figure 1, and spectral ratios for regional P and S are plotted along with results for the geophone array in Figure 3.

The similarity between the three spectral ratios is striking. The modulation observed for near-source geophones appears to be imprinted on both P and S spectral ratios at regional distances. The pattern is an Rg effect in the near-source region because Rg is the dominant wave type up to 10 Hz or so, but must propagate to distance as body waves, as Rg is quickly attenuated. This indicates that strong Rg-to-body-wave scattering is the origin of regional P and S phases for explosions in this area.

The offset between the three spectral ratios appears significant in the lower bands as the P, S, and geophone ratios are separated by just under 0.1 log10 units, P larger than S, and S larger than near-source results. The separation is on the order of the errors, but is consistent across bands.

At high frequencies, all three measurements converge. As pointed out above, the regional S measurement is simply a late P coda measurement at high frequencies, indicating that three different measures of high frequency P all coincide. At the highest frequencies only the near-

source geophones produce measurements, due to larger attenuation effects and lower sample rates for the distant stations.

The similarity in regional P and S spectral ratios violates the "Fisk Conjecture," which states that nuclear explosion corner frequencies are lower for S than for P waves, based on observations for multiple test sites, as described by Fisk (2006). Such an effect, if true, should be observed in SPE results, as the regional S is of high SNR in the anticipated bands (Figure 1), which should cause the S spectral ratio to fall near the notional dashed red curve in Figure 3.

Discussion

Source model comparisons

We test classical explosion source models against the spectral ratio results, using granite media, and the ground truth yields and depths, as well as SPE specific densities and velocities from Rougier and Patton (2015, RP15). The classical models MM71 and DJ91 are constructed using empiricism and theory, both employ cavity radii regressions against variables that include yield, depth and medium parameters, and both postulate a particular form of pressure disturbance at the elastic radius. Moments are related to cavity radii, and corner frequencies are related to elastic radii.

Spectral ratio predictions of the two models are shown in Figure 4. As pointed out by Rougier et al. (2011), Ford and Walter (2013), and Yang (2016), the DJ91 model better predicts moment ratios, while the MM71 model better predicts corner frequencies. Examining the matrix of event pairs, we see that the MM71 model consistently predicts corner frequencies better than the DJ91 model, including corners of the smaller events. The DJ91 model best predicts moment ratios for combinations of SPE-1, -2, and -3, while the MM71 model best predicts those for combinations of SPE-4P and -6, our most extreme events in terms of scaled depth of burial, and some are poorly predicted by both, such as combinations of SPE-5 with SPE-2, -3, and -6.

Because of the different strengths of the MM71 and DJ91 models, it is tempting to substitute the more modern, and better populated cavity radius relationship from DJ91 into the MM71 model (e.g. RP15). If Mueller and Murphy (1971) had access to the DJ91 cavity radius relationship, they might have adjusted other model parameters to compensate, nevertheless, it is of interest to apply this prediction to data, and this is shown in Figure 5. The hybrid model fits nicely in many cases, especially for combinations of SPE-1, -2, and -3; but poorly for ratios involving SPE-6. We conclude that the hybrid model is a reasonable choice for the most over buried events in the Climax Stock source media.

Fisk Conjecture

Fisk (2006) analyzed source spectra from nuclear explosions to show that P spectra have higher frequency corners than S spectra, with differences related to source media velocity ratios. This implies that differences between P and S that we see in discrimination and other work arises from source rather than propagation effects. If this is true, models for shear wave generation by explosions may be based on classical source models. There are many adherents to this idea in the monitoring community. It is of critical importance to understand the S wave generation of explosions because Sg and Lg phases can be large at local and regional distances, and these phases provide discrimination power through P/S and S spectral ratios, and are of interest for yield estimation, especially the codas, which provide high precision measurements.

We see no frequency shift between P and S spectral ratios at regional distances for SPE-3 and SPE-5, thus find no support for the Fisk Conjecture. We do not take similarities between spectral ratios of transverse and other components in near-source data as a violation of the Fisk Conjecture, as the transverse component will be composed of waves of many types traveling many directions due to strong scattering in the source region.

There are ways the Fisk Conjecture could be faulty, including the older propagation models that were used, and the fact that earthquakes, mostly deep sources, were used to construct them. Recent propagation model improvements include constraints on moments and corner frequencies obtained from high quality coda or envelope spectral ratios, as well as allowing source parameters to deviate from constant stress scaling laws in the tomographic inversion procedure. These techniques have improved attenuation models, and provide absolute site terms that can be used to better isolate source spectra.

Secondly, we must tease out differences in attenuation between shallow and deep sources, as the shallow sources may generate surface or guided waves that propagate preferentially in shallow, highly attenuating crustal layers.

Finally, the lack of Fisk Conjecture observations may have something to do with the unusual nature of the SPE experiment tests, their low yields, shallow burial, and large, scaled depths of burial. Many in the monitoring community lean towards the last point, and these issues remain to be resolved.

Source of modulation

The spectral modulations we observe are very distinctive, and are more pronounced for spectral ratios involving the larger events, SPE-5 and SPE-6. We do see subtle modulations for SPE-2 and SPE-3 relative to SPE-1 and SPE-4P, and these are more convincing when viewed side by side with ratios containing the larger events. Modulations are broader in addition to being deeper for the large events, and appear to begin at frequencies as low as 6 Hz.

Spectral modulations can arise from interference effects, such as between Rg generated by the explosion (prompt) and spall (late damage) sources. Depth dependent Rg excitation may also play a role. To examine the latter point, we generated Rg for SPE shots and geophone array locations using wavenumber integration routines from the Computer Programs in Seismology package, applied to layered models found in Rowe and Patton (2015), Pitarka et al. (2015), and Yang (2016). Strong modulations appeared in these spectral ratios, but at frequencies above 20 Hz. This is too high to be consistent with our observations, and will be damped using realistic attenuation, which may be why we don't observe them.

Another issue is whether or not near-source P waves show the modulation. This might occur via phase differences between explosion and prompt damage effects (likely small, of course) or propagation multipathing. We looked at P spectral ratios and deconvolved P wave traces using an empirical Green's function approach to test this. Figure 6 shows waveform examples and spectral ratios in which the observed modulation does not appear.

Thus, we are left with interference between prompt and late time damage, including spall, as the source of the modulation. Preliminary calculations can reproduce the modulation at the observed frequencies, but assume no prompt damage mechanism, which has now been observed (Patton et al, 2018; this volume, also see Stroujkova et al, 2018). Differences between near and far field moments taken at 6-8 Hz, close to modulation bands, are also attributed to this mechanism (Larmat et al, 2017).

Implications for monitoring

Our observations support an interference phenomenon between Rg generated by prompt and late time damage as the source of a distinct modulation in spectral ratios. The same modulation appears in P and S spectral ratios at regional distances, indicating that near source scattering of Rg to P and S body waves is the source of the regional phases we observe for explosions.

Rg to S scattering has long been proposed as a source for regional explosion S, and is supported by modulations observed in lower bands (Gupta et al., 1992; Patton and Taylor, 1995; Gupta and Patton, 2008), and observations that P/S ratios are more effective as discriminants in higher bands (e.g. Fisk, 1996). The latter observation is consistent with increased levels of low frequency regional S due to the Rg to S scattering, because the Rg is more easily excited in the lower bands, leaving the high frequency ratios representing a purer P/S signal.

Our results show that Rg-P scattering is also present in regional P. This does not help us to understand the improvement of P/S ratio discrimination in higher bands, thus we are left with a mystery. We point out that the regional P spectral ratios are derived from much higher SNR portions of the waveforms than are the S spectral ratios, thus the regional P modulation is a strong observation.

Conclusions

The SPE Phase-1 experiments provide a unique opportunity to study low yield, over buried explosions, and unravel source and path effects on seismic waveforms. We have studied spectral ratios based on envelopes of far-field (near source surface geophone array), local and near regional wavefields. Station redundancy via stacking, and use of the direct and coda portions of the envelopes allow us to measure spectral ratios to unprecedented precision, from 1 to 200 Hz.

We observe that the far-field waveforms produce spectral ratios that do not depend on component as R, T, and Z ratios over plot each other, within error bars. This is expected because all components include homogenized wavefields of different wave types traveling different directions, and we do not read a violation of the Fisk Conjecture into these matches.

More convincingly, we do not see evidence of the Fisk Conjecture in the spectral ratio results of P and S at regional distances as these spectral ratios overlay each other. The Fisk Conjecture predicts a lower corner frequency for S spectral ratios, which should be observable if it applies.

The spectral ratios include a distinctive modulation or notch between 6 and 9 Hz, deeper and broader for ratios involving the larger explosions (SPE-5 and SPE-6). The same modulation is observed for both P and S phases at regional distances.

Classical explosion source models MM71 and DJ91 predict the suite of spectral ratio pairs poorly. A hybrid model formed by inserting the more modern and well constrained DJ91 cavity radius into the MM71 model, predicts results reasonably well for all pairs that do not involve SPE-6, the least over buried of the explosion tests.

We have argued that the modulation observed in the near-source region, and for regional P and S phases is produced in the near-source region by interference between Rg wavefields from prompt and late time damage (including spall). This Rg, which is multiply scattered in the source region, is further scattered into P and S body waves that are propagated to regional distances, retaining the Rg modulation imprint. As we see the effect for both P and S phases at regional distances, the scattering origin of these phases does not explain the improved ability of P/S ratios to discriminate between explosions and earthquakes at higher frequencies. This argument works best if S waves are produced by Rg scattering, but not P.

Acknowledgements

The authors are thankful for discussions with Mark Fisk, Sean Ford, Richard Stead, Jessie Bonner, Cathy Snelson, Dave Steedman, and Garrett Euler. This research was supported by the US DOE under contract DE-AC52-06NA25396.

References

Denny, M.D., and L.R. Johnson (1991), The explosion seismic source function: Models and scaling laws reviewed, in Explosion Source Phenomenology, Taylor, S.R., H.J. Patton, and P.G. Richards (Editors), AGU Monograph 65**,** 1–24.

Fisk, M.D., H.L. Gray, and G.D. McCartor (1996), Regional discrimination without transporting thresholds, *Bull. Seism. Soc. Am*. **86**, 1545–1558.

Fisk, M.D. (2006), Source spectral modeling of regional *P*/*S* discriminants at nuclear test sites in China and the former Soviet Union, *Bull. Seism. Soc. Am.*, **96**, 2348–2367, doi:10.1785/0120060023.

Ford, S.R. and W.R. Walter (2013), An explosion model comparison with insights from the Source Physics Experiments, *Bull. Seism. Soc. Am*., **103**, 2937-2945, doi10.1785/0120130035.

Gupta, I.N., W. Chan, and R Wagner (1992), A comparison of regional phases from underground nuclear explosions at East Kazakh and Nevada test sites, *Bull. Seism. Soc. Am*., **82,** 352-382.

Gupta, I.N. and H.J. Patton (2008), Difference spectrograms: A new method for studying S-wave generation from explosions, *Bull. Seism. Soc. Am*., **98**, 2460-2468, doi10.1785/0120080057.

Larmat, C., E. Rougier, and H.J. Patton (2017), Apparent explosion moments from Rg waves recorded on SPE, *Bull. Seism. Soc. Am*., **107**, 43-50.

Mueller, R.A., and J.R. Murphy (1971), Seismic characteristics of underground nuclear detonations, Part I: Seismic spectrum scaling, *Bull. Seism. Soc. Am*., **61,** 1675–1692.

Patton, H.J., and S.R. Taylor (1995), Analysis of *Lg* spectral ratios from NTS explosions: implications for the source mechanisms of spall and the generation of *Lg* waves, *Bull. Seism. Soc. Am*., **85,** 220-236.

Pitarka, A., and 11 co-authors (2015), Analysis of ground motion from an underground chemical explosion, *Bull. Seism. Soc. Am*., **105**, 2390-2410.

Rougier, E., H. J. Patton, E. E. Knight, and C. R. Bradley (2011), Constraints on burial depth and yield of the 25 May 2009 North Korean test from hydrodynamic simulations in a granite medium, *Geophys. Res. Lett*., **38**, L16316, doi:10.1029/2011GL048269.

Rougier, E., and H.J. Patton (2015), Seismic source function from free-field ground motions recorded on SPE: Implications for source models of small, shallow explosions, *J. Geophys. Res*., **120**, 3459-3478, doi10.1002/20124JB011773.

Stroujkova, A. (2018). Rock damage and seismic radiation: A case study of the chemical explosions in New Hampshire, *Bull. Seism. Soc. Am*. 107, doi:10.1785/0120180117.

Yang, X. (2016). Source spectra of the first four Source Physics Experiments (SPE) explosions from the frequency-domain moment-tensor inversion, *Bull. Seism. Soc. Am*. **106**, doi:10.1785/0120150263.

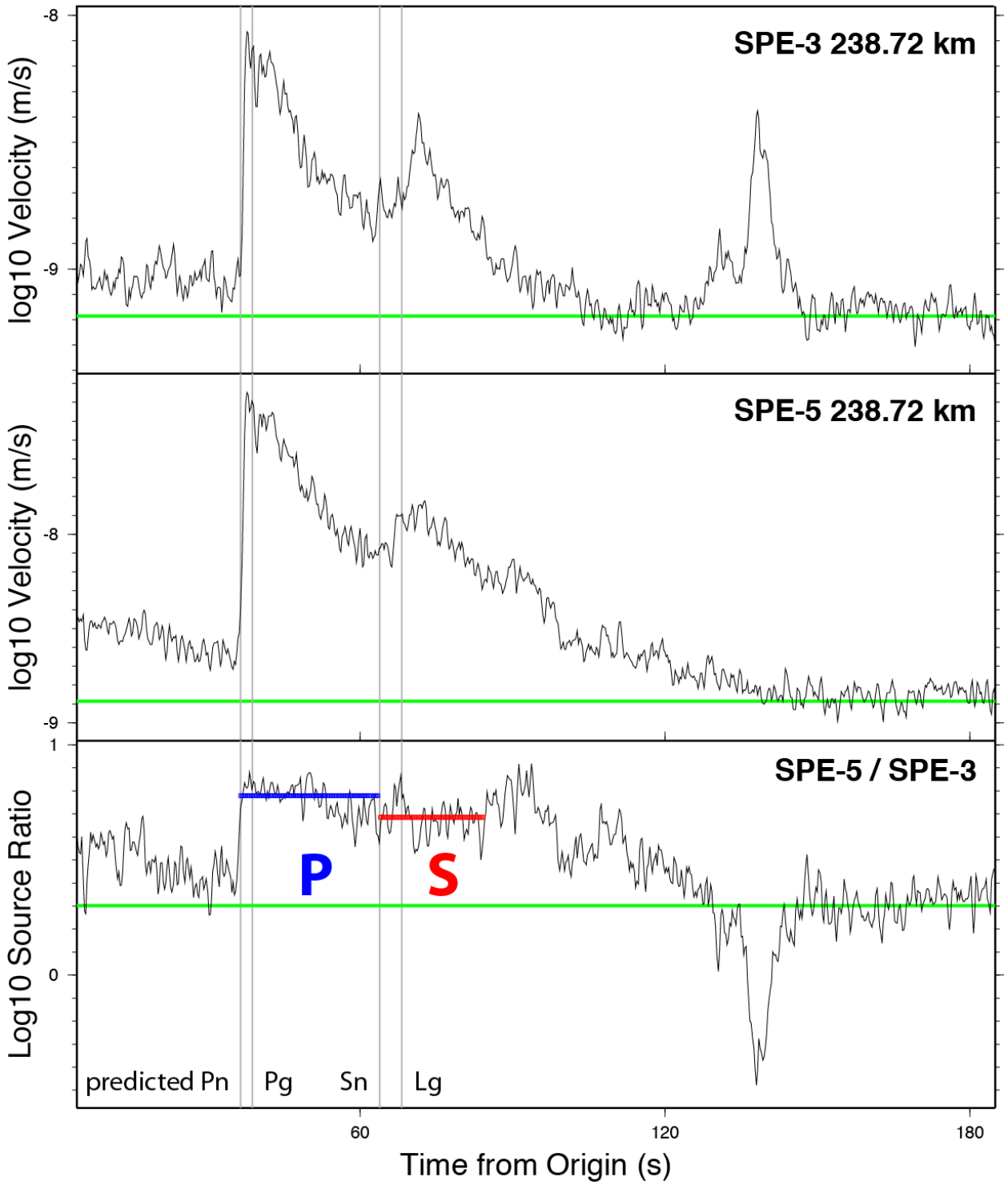

Figure 1. Envelope differencing methodology. Example shows NVAR array, SHZ stack, 8-12 Hz. Ratios are taken point by point over time segments where both envelopes exceed twice the noise level (horizontal green lines). Vertical gray lines represent predicted arrivals. Note that the unassociated signal in the SPE-3 envelope is easily ignored by the measurement script.

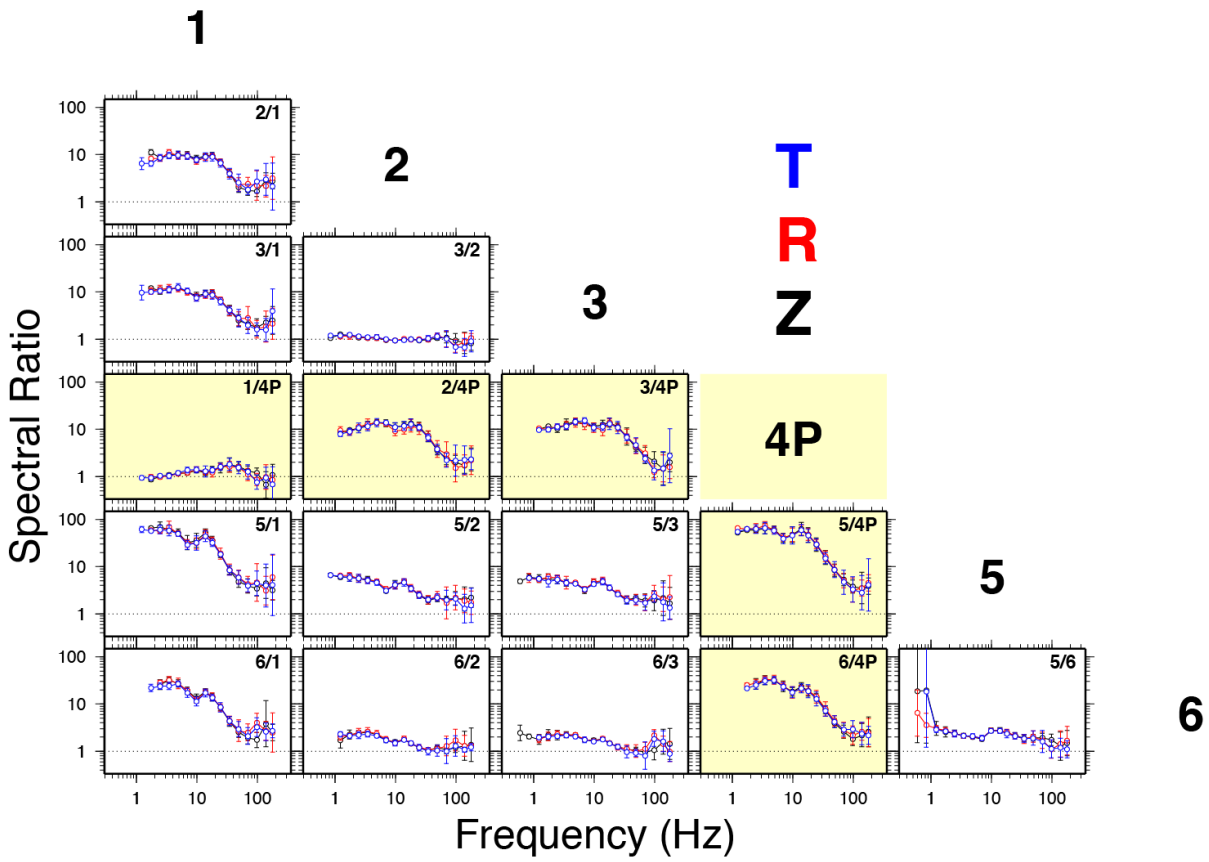

Figure 2. Coda spectral ratios, all SPE Phase 1 pairs. The event with the larger yield is in the numerator, except for 2 versus 3 where we made an arbitrary choice. Blue, red, and black represent transverse, radial, and vertical components, respectively. Blue (T) is plotted on top, over red (R), both over black (Z). Error bars represent twice the standard deviation of stacked spectral ratios, as measured by the MADn. SPE-4P is considered the Green's function event for Phase 1; this is emphasized by the yellow backgrounds.

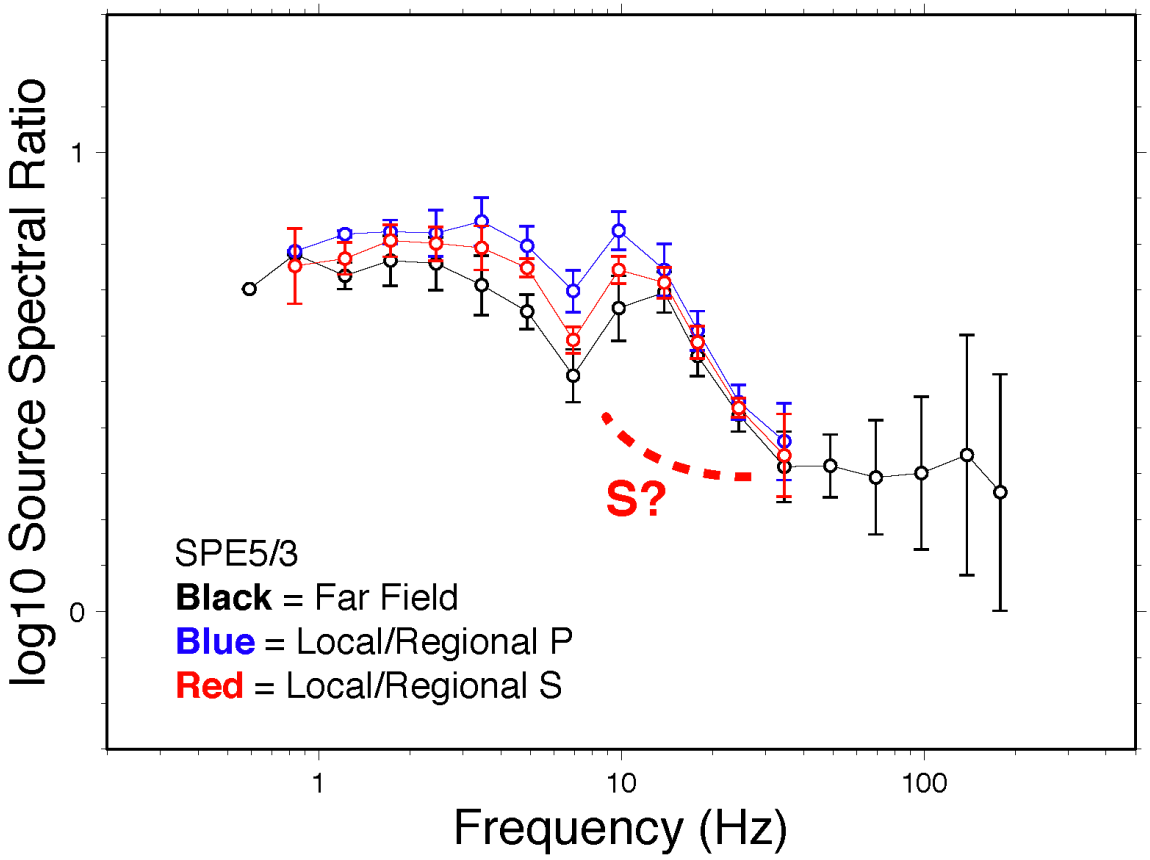

Figure 3. Spectral ratios for SPE-5 and SPE-3 at near-source (labeled as far field) and regional distances for P and S, colored black, blue and red, respectively as indicated by the legend. The near-source result is taken from Figure 2, vertical component. The notional track of the S spectral ratio given the Fisk Conjecture is shown by the dashed red line.

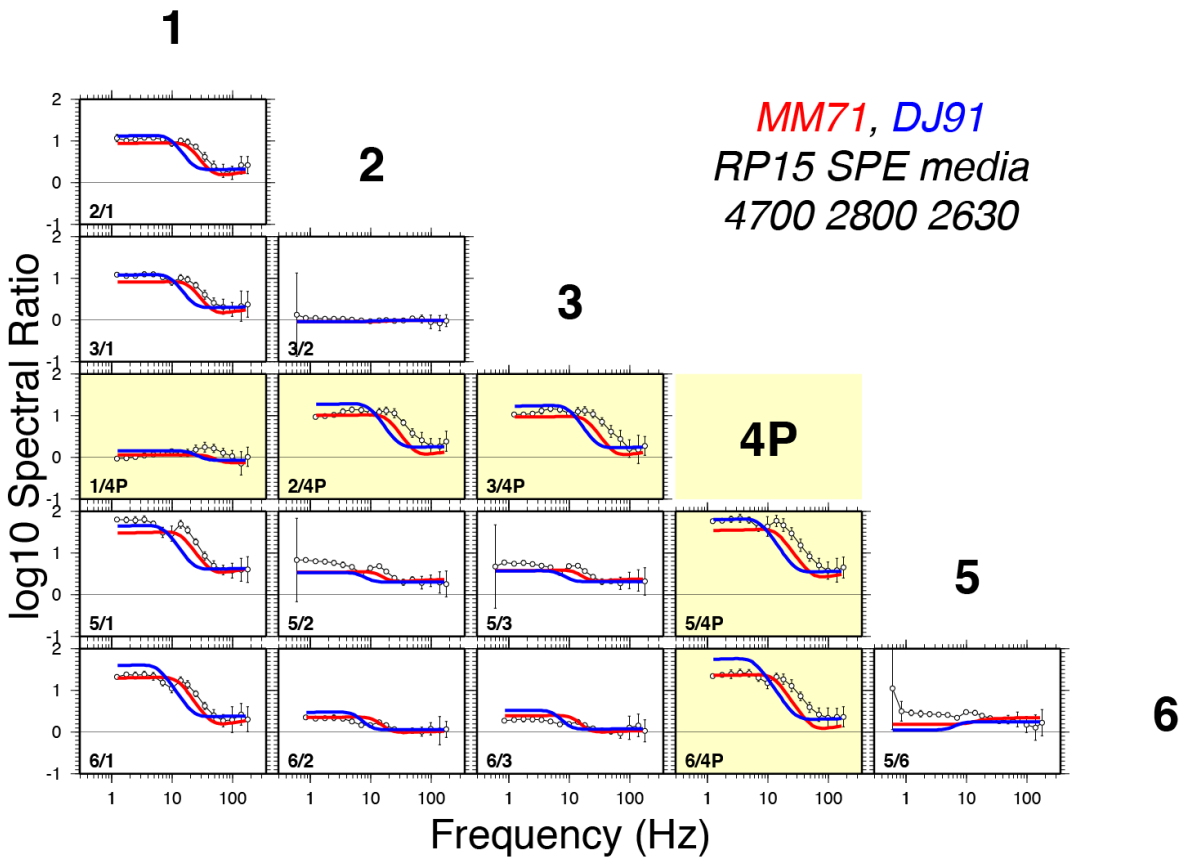

Figure 4. Vertical component spectral ratios along with MM71 (red) and DJ91 (blue) predictions.

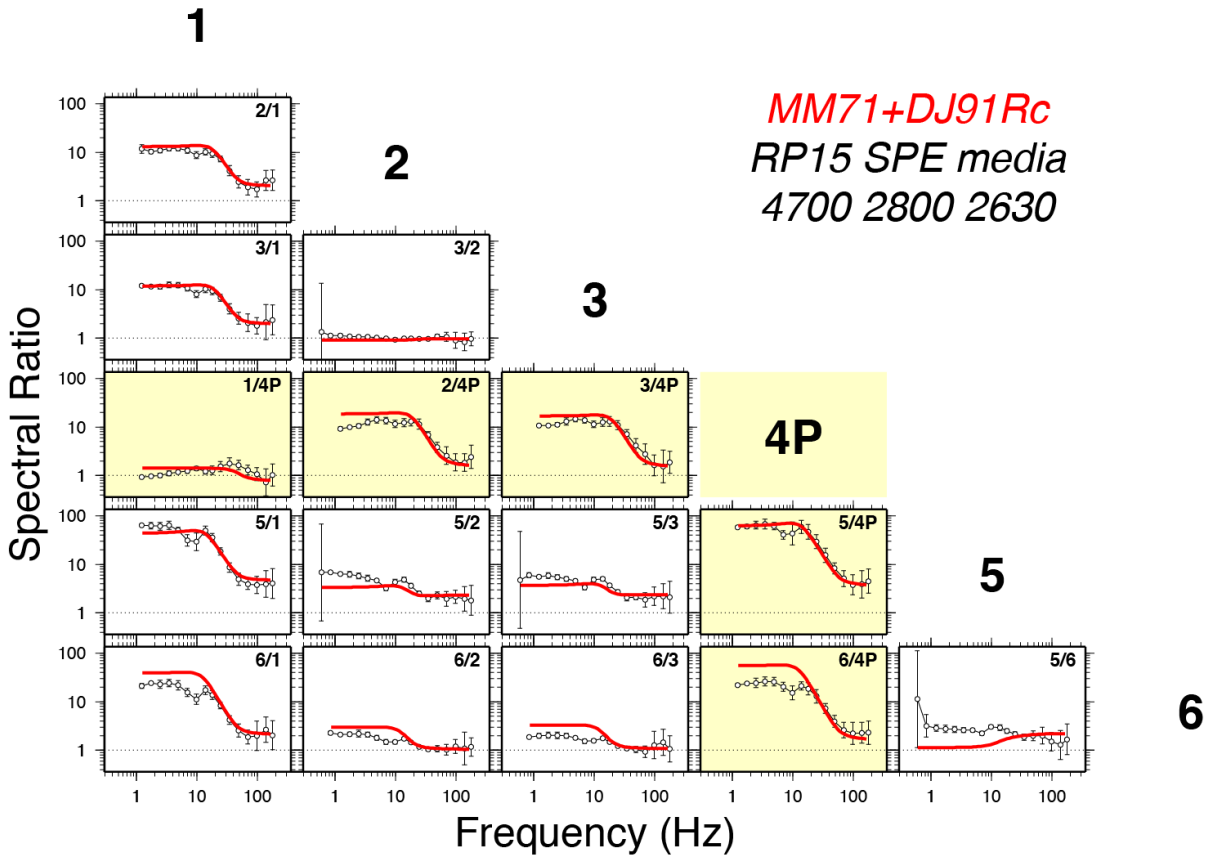

Figure 5. Vertical component spectral ratios along with predictions of the hybrid source model created by inserting the DJ91 cavity radius into the MM71 model.

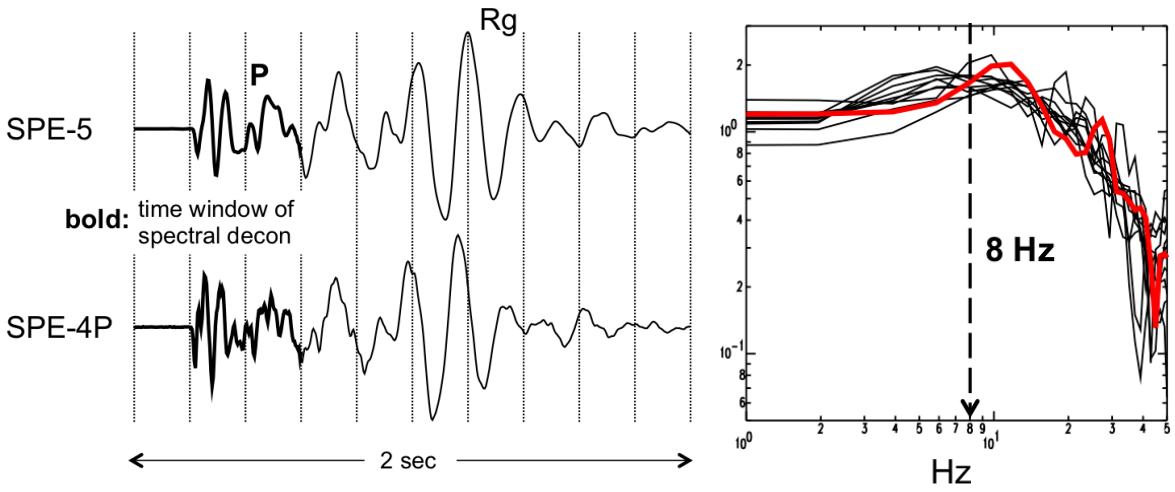

Figure 6. Example P wave segments from station L1018 used in spectral ratio and deconvolution procedures for SPE-5 and SPE-4P (left), and SPE-5 / SPE-4P spectral ratios for near-source geophone array P segments (right). The red spectral ratio represents the time domain deconvolution example, the remaining spectral ratios were constructed using standard frequency domain methods.